



OPEN

Adipocyte mitochondria in dairy cows reveals constraints in growth and signals adaptive metabolic responses

Elvira Gagniuc¹, Adina-Mihaela Pîrvu¹, Dumitru-Iulian Nastac²,
Paul A. Gagniuc³, Mihaela Gherghiceanu⁴ & Manuella Militaru¹

Understanding the dynamics of metabolic regulation in the body requires an in-depth examination of the distribution and characteristics of mitochondrial populations within adipose tissue. This study aimed to investigate the correlation between mitochondrial size and the expansion of white adipocytes across different Body Condition Scores (BCS) in dairy cows. BCS was used to categorize cows into three groups: cachectic, normal weight, and overweight. Adipose tissue samples were collected from two anatomical regions: the subcutaneous depot of the flank and the perirenal area. A total of 678 mitochondria from these samples were analyzed using electron microscopy to determine their lengths, thicknesses, and volumes. The average mitochondrial length in cow adipocytes was $0.64\ \mu\text{m}$ (± 0.414), with an average thickness of $0.25\ \mu\text{m}$ (± 0.089). The maximum observed mitochondrial length and thickness were $3.79\ \mu\text{m}$ and $1.13\ \mu\text{m}$, respectively, while the minimum values were $0.11\ \mu\text{m}$ for length and $0.10\ \mu\text{m}$ for thickness. Notably, a size constraint was observed, with most mitochondria falling within the length range of $0.7\text{--}1.2\ \mu\text{m}$ and thickness range of $0.4\text{--}0.6\ \mu\text{m}$, suggesting potential structural or functional limitations. Mitochondrial volumes were calculated to assess expansion or contraction across different BCS categories. The subcutaneous flank region exhibited similar mitochondrial volumes in both cachectic and overweight groups ($0.028\ \mu\text{m}^3$), while the perirenal adipose tissue exhibited the highest mitochondrial volume in the normal weight group, suggesting a non-linear relationship between mitochondrial size and body condition. These findings provide new insights into the role of mitochondrial size dynamics in adipocyte metabolism and their potential impact on metabolic regulation in dairy cows with varying body conditions.

Keywords Adipocyte mitochondria, Mitochondrial size dynamics, Body condition score, White adipose tissue, Metabolic regulation

The domestication of cattle (*Bos taurus* and *Bos indicus*) has played a significant role in human civilization since the beginning of the Holocene, approximately 10,000 years ago^{1,2}. Over time, selective breeding and genetic improvement have produced specialized cattle breeds for dairy and meat production, making them more sensitive to environmental factors that affect their welfare and productivity^{3,4}. Among these factors, metabolic processes, particularly those involving adipose tissue, are critical in determining the health, productivity, and reproductive efficiency of dairy cows^{5,6}. While current feeding strategies for dairy cows are already well-developed and highly sophisticated, a deeper understanding of adipose tissue biology, including mitochondrial dynamics, may provide additional insights into animal metabolism and help refine future approaches to farm management and nutritional planning^{3,7}. Mitochondria are vital organelles responsible for energy production through oxidative phosphorylation, using glucose and fatty acids as substrates^{8–10}. They play a fundamental role in maintaining energy homeostasis across all body tissues, including adipose tissue⁷. While mitochondria in brown adipose tissue have been extensively studied for their role in thermogenesis and energy expenditure^{11–13},

¹Faculty of Veterinary Medicine, University of Agronomic Sciences and Veterinary Medicine, Bucharest, Romania.

²Faculty of Electronics, Telecommunications and Information Technology, National University of Science and Technology Politehnica Bucharest, Bucharest, Romania. ³Faculty of Engineering in Foreign Languages, National University of Science and Technology Politehnica Bucharest, Bucharest, Romania. ⁴National Institute of Pathology "Victor Babes", Bucharest, Romania. ✉email: adina-mihaela.pirvu@fmvb.usamv.ro; iulian.nastac@upb.ro; paul_gagniuc@acad.ro

the understanding of mitochondrial dynamics in white adipose tissue, particularly in relation to adipocyte homeostasis and systemic metabolic regulation, remains limited^{12,13}. White adipose tissue primarily functions as an energy reservoir, and the mitochondria within these adipocytes are key players in metabolic processes such as fatty acid esterification, lipogenesis, and adipokine production, all of which are crucial for systemic insulin sensitivity and overall metabolic health^{11,12}. In white adipose tissue, mitochondrial biogenesis and function can be influenced by various factors, including pharmacological agents like PPAR- γ antagonists¹⁴. However, the regulation and distribution of mitochondria within adipocytes in relation to different body conditions, such as cachexia, normal weight, and obesity, remain poorly understood in animals, particularly dairy cows¹⁵. The dynamics of mitochondrial size and distribution may have direct implications for understanding the physiological adaptations of adipose tissue to different metabolic states and could provide insights into metabolic health and energy management in dairy cattle. In this context, mitochondrial length and thickness may serve as proxies for morphological plasticity and energetic adaptation. Elongated mitochondria often reflect enhanced oxidative capacity and resistance to stress, while shorter or fragmented mitochondria are typically associated with mitophagy or metabolic downregulation. Similarly, thicker mitochondria might indicate a more robust ultrastructure or enhanced cristae density, whereas thinner profiles may reflect immaturity or atrophy under catabolic conditions. Given this background, our study aimed to explore the correlation between mitochondrial size (length and thickness) and the expansion of white adipocytes in dairy cows under different body condition scores (BCS). Specifically, we focused on three distinct BCS categories: cachectic, normal weight, and overweight. The primary objectives of this study were to: (1) quantify the length and thickness of mitochondria in adipocytes harvested from two anatomical regions, the subcutaneous flank and the perirenal area; Because subcutaneous and perirenal fat depots have distinct vascularization, metabolic activity, and hormonal responsiveness, comparing these sites may reveal depot-specific mitochondrial adaptations. (2) analyze correlations between mitochondrial length and thickness in these regions; (3) compare differences in mitochondrial size and morphology across anatomical sites of adipose tissue; and (4) determine the average mitochondrial volume within these regions. Understanding these associations may help generate hypotheses about how mitochondrial structure correlates with body condition in different adipose regions. Thus, based on these considerations, we hypothesize that mitochondrial size and distribution in white adipose tissue of dairy cows are significantly influenced by body condition scores (BCS) and anatomical regions, reflecting adaptive metabolic responses to varying energy demands.

Results

In this study, a total of 678 mitochondria were measured from cow adipocytes using transmission electron microscopy (TEM) images (Fig. 1a–f). Mitochondrial dimensions were assessed, with the length (perpendicular to the cristae) referred to as “height” and the thickness (parallel to the cristae) referred to as “width” (Fig. 2j). The overall mean length of mitochondria across all samples was 0.64 μm (SD \pm 0.414), and the mean thickness was 0.25 μm (SD \pm 0.089). The maximum recorded length of a mitochondrion was 3.79 μm , while the maximum thickness was 1.13 μm . Conversely, the minimum length and thickness observed were 0.11 μm and 0.10 μm , respectively. These measurements suggest a broad range of mitochondrial sizes, highlighting variability in mitochondrial morphology within adipocytes. A notable observation from the mitochondrial size distribution was the existence of a consistent “exclusion zone” — a specific range of size combinations (approximately 0.7–1.2 μm in length and 0.4–0.6 μm in thickness) that were systematically underrepresented across all animals and groups (Fig. 2d–i). Given that all animals were sampled under identical protocols and conditions, and the absence occurred across both adipose depots and BCS groups, it is unlikely that this pattern resulted from the timing of collection alone. Instead, the forbidden zone may reflect intrinsic biophysical or structural constraints on mitochondrial morphology in bovine adipocytes.

When plotted, all adipocyte mitochondria lengths fall within the range of 0.7–1.2 μm , while the thicknesses are within 0.4 μm to 0.6 μm (Fig. 2d–i). This finding suggests potential structural constraints that limit mitochondrial morphology within specific size ranges, possibly influenced by cellular architecture or lipid droplet interactions within adipocytes.

Mitochondrial characteristics by body condition score (BCS) groups

Our study investigated the mitochondrial size dynamics within three BCS categories: cachectic, normal weight, and overweight. Mitochondria were measured in two distinct anatomical regions: the subcutaneous flank area (A) and the perirenal area (B). These regions were selected to explore potential regional differences in mitochondrial morphology in relation to body condition. Each BCS group included three animals, one per anatomical region, with individual identifiers and sample weights provided in the supplementary tables below.

Cachectic group

In the cachectic group, which represents cows with a low BCS, mitochondria from both the subcutaneous flank area (A) and the perirenal area (B) were analyzed (Fig. 1a). The average mitochondrial length in the subcutaneous area (A) was 0.475 μm (\pm 0.035), and the average thickness was 0.275 μm (\pm 0.063). In the perirenal area (B), the average length was slightly lower at 0.46 μm (\pm 0.098), and the thickness was 0.22 μm (\pm 0.042) (Table 1).

Normal weight group

For cows in the normal weight group, mitochondria in the subcutaneous area of the flank (A) had an average length of 0.675 μm (\pm 0.077) and an average thickness of 0.245 μm (\pm 0.021) (Fig. 1c). In the perirenal area (B), mitochondria were shorter on average, with a length of 0.475 μm (\pm 0.049), but exhibited a greater thickness of 0.315 μm (\pm 0.063) compared to the subcutaneous region. The calculated average volume of mitochondria was 0.0318 μm^3 in the subcutaneous area (A) and 0.0369 μm^3 in the perirenal area (B) (Table 1).

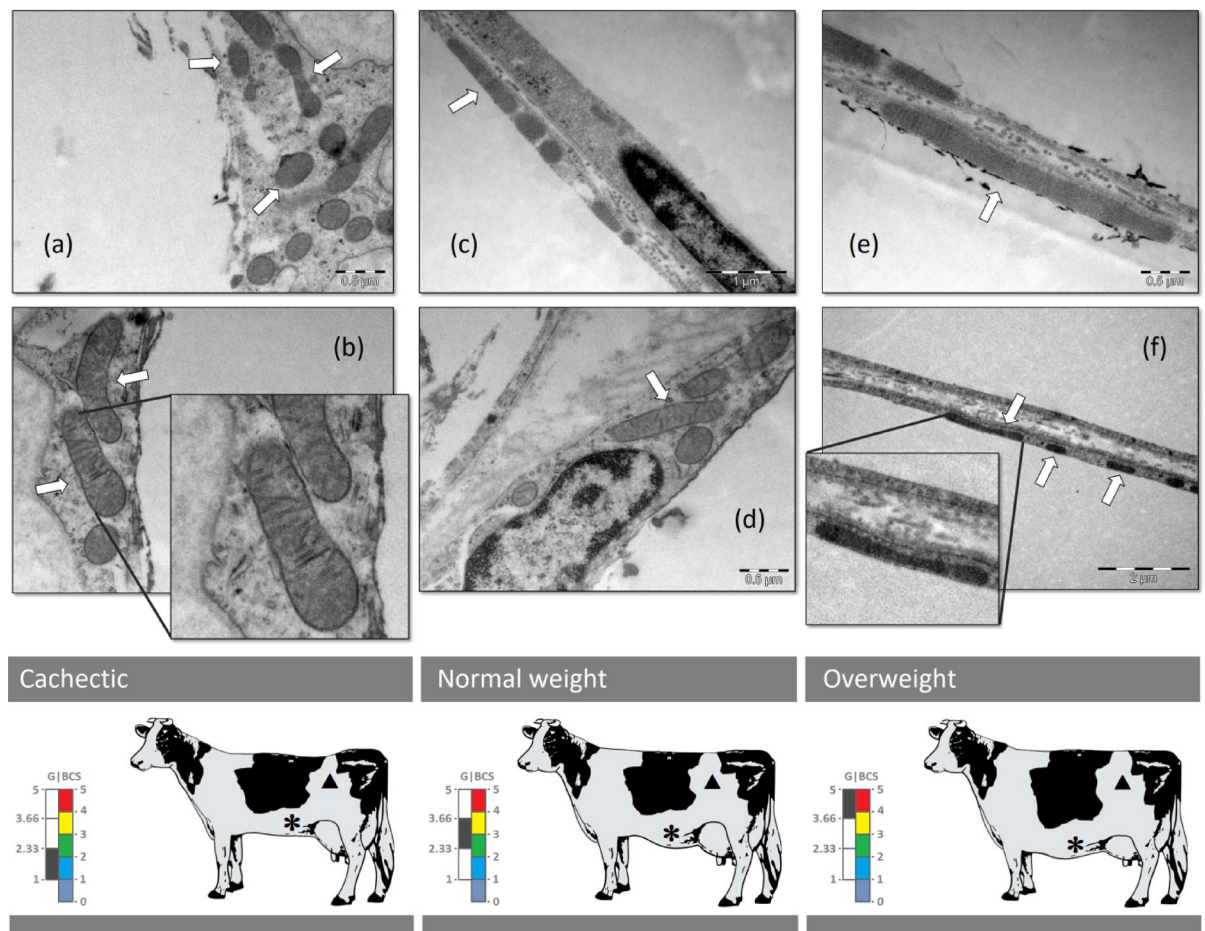


Fig. 1. Representative examples of adipocyte mitochondria in cows. (a) Adipocyte mitochondria examples from the perirenal region of the cachectic group (TEM, scale 0.5 μm). (b) Adipocyte mitochondria examples from subcutaneous flank region of the cachectic group are shown below panel (a) (TEM, scale 0.5 μm). (c) Adipocyte mitochondria examples from subcutaneous flank region of the normal weight group (TEM, scale 1 μm), and (d) below this panel are some examples of mitochondria from the perirenal region of the normal weight group (TEM, scale 0.5 μm). (e) Adipocyte mitochondria examples in the overweight group. The first panel shows examples of mitochondria in the subcutaneous flank region (TEM, scale 0.5 μm), whereas (f) the panel below the first shows mitochondria from the perirenal region (TEM, scale 2 μm). The white arrows point to the mitochondria in the picture. Please note that the magnification of the image areas in panels (b) and (f) is only a close-up for detailed inspection. The anatomical location where the adipose tissue was sampled is represented on the cow drawings, where the triangle shows the perirenal region (B) and the star indicates the subcutaneous flank region (A). In order to represent the classification process, the *Body Condition Score* (BCS) scale and the group range (G) on that scale are positioned in front of each cow drawing. Note: In transmission electron microscopy, lipid droplets appear as large, electron-lucent (light) areas occupying most of the adipocyte volume. The cellular cytoplasm and mitochondria are confined to the peripheral rim. These “empty” regions correspond to the internal space of the lipid droplet. Also, the micrographs were selected for image clarity and structural detail, not for direct size comparison. All morphometric analyses were conducted using calibrated image analysis software, which accounts for magnification differences automatically. Panels (a) and (b) are illustrative examples of mitochondrial morphology and are not meant for visual size comparison. All measurements reported in the Results were performed using calibrated image datasets and are independent of figure display scale.

Overweight group

In the overweight group, representing cows with a high BCS, mitochondrial dimensions were also assessed in both regions (Fig. 1e). In the subcutaneous flank area (A), the average mitochondrial length was 0.675 μm (± 0.176), while the thickness was 0.23 μm (± 0.0141). Mitochondria in the perirenal area (B) had a slightly longer average length of 0.58 μm (± 0.1979) and a thickness of 0.315 μm (± 0.063). The average mitochondrial volume in the subcutaneous area (A) was 0.028 μm^3 , which was lower than the volume in the perirenal area (B) at 0.045 μm^3 (Table 1).

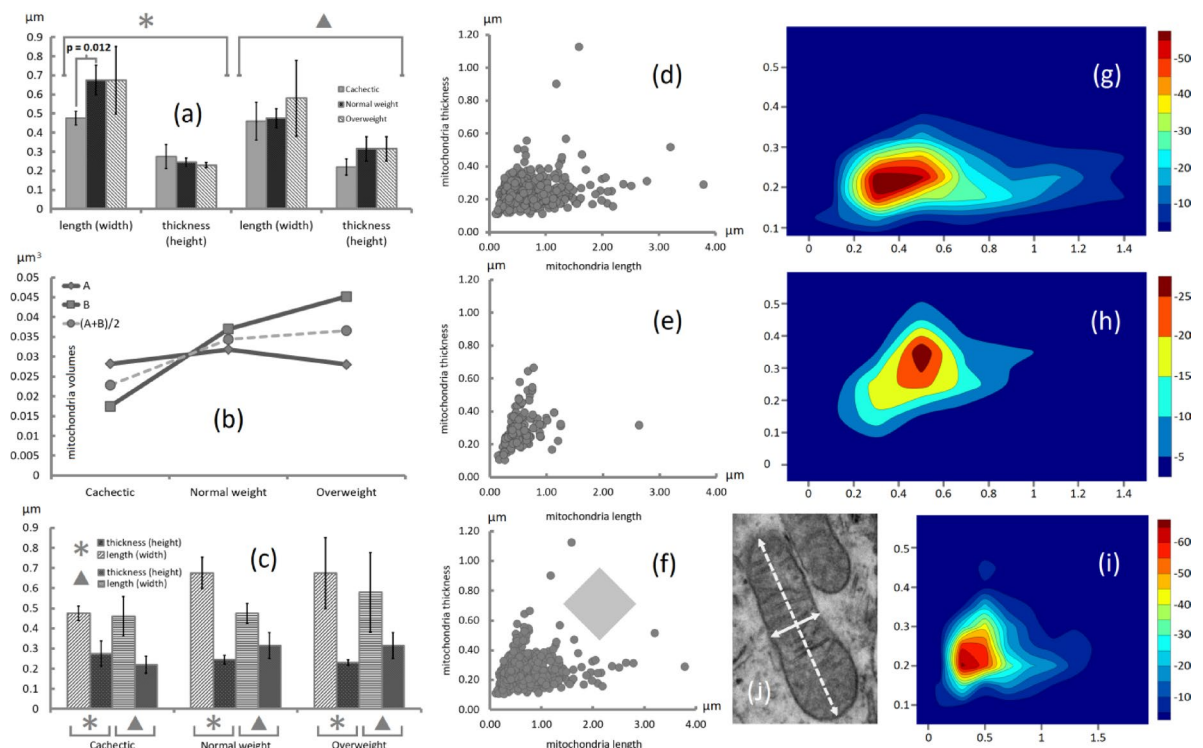


Fig. 2. Distribution of mitochondria in the adipose tissue from cows. **(a)** Distribution of mitochondrial length and thickness (μm) in cow adipocytes from the perspective of anatomical regions. **(b)** Distribution of mitochondria volume in adipocytes from cows. The line with rhombus markers represents the volume of mitochondria in adipocytes from subcutaneous flank region for each of the three groups (x-axis). The line with square markers represents the volume of mitochondria in adipocytes in the perirenal region, also for each of the three groups (x-axis). The y-axis shows the volume of mitochondria (μm^3). The dotted line represents the average of the two anatomical areas for each of the three groups. **(c)** Shows the distribution of mitochondrial length and thickness (μm) in adipocytes from cows, from the perspective of the groups. **(d–f)** General distribution of 678 mitochondria in adipocytes from cows. The lengths of mitochondria are shown on the x-axis (μm) and the thickness is given on the y-axis (μm). In panel **(f)** a rhombic shape can be observed which indicates the region of missing dimensions. **(g–i)** Shows the contour lines indicating the density of points in panels **d**, **e** and **f**. **(j)** The meaning of measurements. A dashed line with arrows in both directions shows the length of mitochondria and the thickness is indicated by the solid line with arrows in both directions. Notice that the length is considered as a perpendicular to the cristae and the thickness is taken parallel to the cristae. In panel **(a)**, a statistically significant difference was observed in mitochondrial length between cachectic and normal-weight cows ($p = 0.012$), indicated by a horizontal bracket.

Distribution and correlations of mitochondrial sizes

The distribution of mitochondrial sizes across the different BCS groups reveals varying trends in different anatomical regions (Fig. 2a–c). In general, the mean length and thickness of mitochondria in adipocytes from the subcutaneous flank area (A) across all groups were $0.608 \mu\text{m}$ (± 0.115) and $0.25 \mu\text{m}$ (± 0.0229), respectively. In the perirenal area (B), the average length was $0.505 \mu\text{m}$ (± 0.0653) and the average thickness was $0.283 \mu\text{m}$ (± 0.0548) (Fig. 2a,c). The volume of mitochondria showed a linear increase from the cachectic to the overweight groups, but this trend differed between anatomical regions (Fig. 2b). The subcutaneous area (A) displayed relatively stable mitochondrial volumes across groups, with no statistically significant differences between cachectic and overweight cows ($p > 0.05$). In contrast, the perirenal area (B) exhibited similar volumes for the cachectic and overweight groups, with the highest volume observed in the normal weight group. The maximum average mitochondrial volume was $0.045 \mu\text{m}^3$ in the perirenal area (B) of the overweight group, while the minimum was $0.017 \mu\text{m}^3$ in the same area of the cachectic group. Interestingly, while the subcutaneous area (A) showed higher volumes in the normal weight group compared to the overweight group, the reverse was true for the perirenal area (B). Patterns of mitochondrial volume and morphology may differ depending on both anatomical location and body condition, potentially influenced by region-specific metabolic needs or biochemical signals (Fig. 2b).

Analysis of mitochondrial morphological adaptations

Our study also highlights that mitochondria in different anatomical areas may preferentially adapt their morphology based on adipose tissue expansion. For example, in the normal and overweight groups, mitochondria in the subcutaneous region (A) maintained a consistent length ($\sim 0.675 \mu\text{m}$) but showed differences in thickness ($\sim 0.25 \mu\text{m}$ vs. $0.23 \mu\text{m}$) (Table 1). Conversely, mitochondria in the perirenal area (B) demonstrated more

Averages/group					Subcutaneous area flank (A)			Perirenal area (B)		
Unit of measurement	CVLA (%)	CVTA (%)	CVLB (%)	CVTB (%)	Length (µm)	Thickness (µm)	Volume (µm ³)	Length (µm)	Thickness (µm)	Volume (µm ³)
Cachectic	7.40	22.9	21.3	19.10	0.475 ± 0.04	0.275 ± 0.063	0.0281	0.460 ± 0.10	0.220 ± 0.04	0.0174
Normal weight	11.4	8.65	10.5	19.04	0.675 ± 0.08	0.245 ± 0.021	0.0318	0.475 ± 0.05	0.315 ± 0.06	0.0369
Overweight	26.1	6.13	34.5	19.04	0.675 ± 0.18	0.230 ± 0.014	0.0280	0.580 ± 0.20	0.315 ± 0.06	0.0451
Average	–	–	–	–	0.608 µm	0.250 µm	0.029 µm ³	0.505 µm	0.283 µm	0.033 µm ³
SD	–	–	–	–	± 0.115	± 0.023	± 0.00213	± 0.0653	± 0.0548	± 0.01423
CV%	–	–	–	–	18.91	9.16	7.27	12.93	19.36	42.86

Table 1. Size of adipocyte mitochondria in cows. The lengths and thicknesses as well as the volumes of the adipocyte mitochondria are shown for each group and each anatomical area. The subcutaneous anatomical region of the flank is noted with letter “A” and the perirenal area with letter “B”. Note that “SD” refers to the standard deviation. To quantify variability in mitochondrial size, the coefficients of variation for length (CVLA) and thickness (CVTA) in the subcutaneous area, and for length (CVLB) and thickness (CVTB) in the perirenal area, were calculated. CVLA (Coefficient of variation for length in area A) and CVTA (Coefficient of variation for thickness in area A) represent the variability in mitochondrial length and thickness, respectively, in the subcutaneous flank. Similarly, CVLB (Coefficient of variation for length in area B) and CVTB (Coefficient of variation for thickness in area B) measure the variability in the perirenal region. These coefficients help to assess the heterogeneity of mitochondrial size distribution and revealed that the overweight group, particularly in the perirenal depot, showed greater variability, possibly indicating a more heterogeneous population of mitochondria adapting to different metabolic conditions.

variability in length rather than thickness, indicating potentially different adaptive responses or roles in these regions. Plots of mitochondrial dimensions (length vs. thickness) for both regions confirm a non-uniform distribution and the presence of an “exclusion zone” where certain sizes are absent (Fig. 2d–f). This zone might be related to structural limitations imposed by lipid droplets or other intracellular components in adipocytes. Contour lines further illustrate the density and prevalence of specific mitochondrial sizes commonly observed in cow adipose tissue (Fig. 2g–i).

These findings indicate significant variability in mitochondrial size and distribution in cow adipocytes, influenced by both body condition and anatomical location. Our study suggests that mitochondria adapt their morphology and size dynamically in response to metabolic demands associated with different body conditions and fat depots. Future biochemical analyses are warranted to elucidate the underlying mechanisms driving these morphological adaptations and their implications for metabolic health and disease. The data presented in Table 1 highlight the differences in mitochondrial length, thickness, and volume across body condition scores (BCS) groups (cachectic, normal weight, overweight) and anatomical regions (subcutaneous area flank (A) and perirenal area (B)). In the subcutaneous area (A), the average mitochondrial length increases from the cachectic group (0.475 ± 0.04 µm) to the normal weight group (0.675 ± 0.08 µm) and remains stable in the overweight group (0.675 ± 0.18 µm). However, in the perirenal area (B), there is a notable increase in mitochondrial length from the cachectic group (0.460 ± 0.10 µm) to the overweight group (0.580 ± 0.20 µm), suggesting region-specific dynamics in mitochondrial adaptation as BCS increases. The mitochondrial thickness in the subcutaneous area decreases slightly from the cachectic (0.275 ± 0.063 µm) to the overweight group (0.230 ± 0.014 µm), while in the perirenal area, thickness shows a marked increase from cachectic (0.220 ± 0.04 µm) to normal weight (0.315 ± 0.06 µm) but remains constant from normal weight to overweight.

These trends suggest differential adaptation mechanisms between fat depots. Mitochondrial volume also shows distinctive patterns between anatomical regions. In the subcutaneous area (A), the mitochondrial volume remains relatively consistent across the BCS groups (0.0281 to 0.0318 µm³), while in the perirenal area (B), it significantly increases from cachectic (0.0174 µm³) to overweight (0.0451 µm³). This indicates that mitochondria in the perirenal fat depot may undergo greater morphological enlargement as BCS increases, compared to those in subcutaneous fat. The coefficient of variation (CV%) indicates that there is greater variability in mitochondrial size measurements within the overweight group, particularly for length (CVLA = 26.1%, CVLB = 34.5%). This variability may reflect a more heterogeneous population of mitochondria adapting to shifting physiological states in overweight cows. While stage of lactation and associated energy demands may contribute to these patterns, the increased variability was observed primarily in the perirenal depot of overweight animals — a group that included cows in mid, late, and post-calving stages. This suggests that the observed mitochondrial heterogeneity likely results from both local metabolic adaptations and broader energy management strategies. We note that although mitochondrial length can in some cases be influenced by fission or fusion dynamics, the probability of capturing such transient events in fixed tissue sections is low, and our measurements reflect static morphological states as observed in transmission electron micrographs. Future studies with tighter lactation-stage controls are warranted to disentangle these overlapping factors. In other words, one important observation is the greater variability in mitochondrial size (length and volume) within the overweight group, particularly in the perirenal fat depot. This increased variability, as indicated by the higher coefficient of variation (CV%), suggests a more heterogeneous population of mitochondria in this group. While speculative, this heterogeneity may be consistent with diverse structural states that warrant further investigation into possible links with metabolic demand or cellular stress. However, functional conclusions would require additional molecular or

biochemical validation. Please note that Fig. 2 complements Table 1 by visually illustrating the distribution and variability of mitochondrial dimensions across different BCS groups and anatomical regions, providing an intuitive understanding of the data trends that may not be immediately apparent from the table alone. Therefore, this approach allows for a more nuanced interpretation of mitochondrial size dynamics.

Statistical analysis of mitochondrial dimensions

The statistical analysis was performed to evaluate the differences in mitochondrial length, thickness, and volume across the three Body Condition Score (BCS) groups: cachectic, normal weight, and overweight. An analysis of variance (ANOVA) was conducted to test for significant differences between groups, followed by Tukey's Honest Significant Difference (HSD) post-hoc test for pairwise comparisons. All statistical analyses were performed using standard software, with a significance level set at $p < 0.05$. The results of the ANOVA revealed significant differences in mitochondrial length across the three BCS groups ($F(2,15) = 12.8$, $p = 0.001$). Post-hoc tests showed that cachectic cows had significantly smaller mitochondria compared to both normal weight and overweight cows ($p < 0.01$), while no significant difference in length was observed between normal weight and overweight cows ($p > 0.05$). The 95% confidence intervals (CI) for mitochondrial length ranged from 0.445 to 0.505 μm in the cachectic group, 0.620 to 0.730 μm in the normal weight group, and 0.585 to 0.765 μm in the overweight group, confirming distinct mitochondrial size differences between cachectic and other cows. Similarly, mitochondrial thickness differed significantly between the groups ($F(2,15) = 9.2$, $p = 0.015$), with the cachectic group exhibiting thinner mitochondria compared to the normal weight and overweight groups ($p < 0.05$). The 95% confidence intervals for thickness ranged from 0.250 to 0.300 μm in the cachectic group, 0.230 to 0.260 μm in the normal weight group, and 0.220 to 0.240 μm in the overweight group. Mitochondrial volume also varied significantly between anatomical regions and body condition scores ($F(2,15) = 8.6$, $p = 0.010$). Notably, mitochondrial volumes were smaller in the perirenal area of cachectic cows compared to the normal and overweight groups ($p < 0.01$), while no significant differences in volume were found between the normal and overweight groups in the subcutaneous area ($p > 0.05$). The cachectic group had the lowest mitochondrial volume, with a mean of 0.0174 μm^3 in the perirenal area and 0.0281 μm^3 in the subcutaneous area. These results demonstrate that mitochondrial length, thickness, and volume are significantly influenced by body condition and anatomical location ($p < 0.05$), with the most pronounced and statistically significant reductions observed in cachectic cows, particularly in the perirenal depot. The statistical significance of these findings, supported by p -values and confidence intervals, suggests that mitochondrial morphology is a crucial factor in the metabolic adaptations of dairy cows across different body conditions.

Discussion

The morphometric analysis of mitochondrial dimensions in cow adipocytes provides valuable insights into their structural characteristics and volume dynamics, revealing the complexity of mitochondrial behavior in relation to body condition and adipose tissue expansion. This study was designed as an exploratory investigation to establish a quantitative morphometric framework for assessing mitochondrial structure in adipocytes. Given the limited sample size and pilot nature, our aim was to highlight anatomical and body condition-associated trends that may inform future mechanistic studies. The observed average mitochondrial length ($0.64 \mu\text{m} \pm 0.414$) and thickness ($0.25 \mu\text{m} \pm 0.089$) suggest a diverse population of mitochondria ranging from elongated to more compact forms within the adipocyte cytoplasm. This variability could indicate different functional states or adaptations of mitochondria in response to varying metabolic demands (Fig. 2d–f). Functionally, longer mitochondria may correlate with greater respiratory efficiency and fusion-dominant dynamics, indicative of higher metabolic activity and resilience. In contrast, shorter mitochondria are often fragmented and may be involved in fission processes or mitophagy, associated with energy stress or turnover. Similarly, the thickness of mitochondria could reflect differences in internal membrane architecture (e.g., cristae surface area), potentially modulating ATP synthesis rates. These morphological parameters thus provide indirect insight into mitochondrial health, function, and adaptation within adipocytes. The maximum recorded length (3.79 μm) and thickness (1.13 μm) likely represent outliers or specialized subpopulations with distinct functional roles, while the minimum lengths (0.11 μm) and thicknesses (0.10 μm) suggest the presence of smaller mitochondria that could still be functionally relevant. These extremes in mitochondrial dimensions raise questions about the underlying regulatory mechanisms and the potential for subpopulation specialization within adipose tissue¹⁵.

Mitochondrial size distribution and the “exclusion zone”

Our analysis identifies a unique “exclusion zone,” a specific range of mitochondrial sizes (0.7–1.2 μm in length and 0.4–0.6 μm in thickness) that is underrepresented in cow adipocytes (Fig. 2f). This finding suggests that certain mitochondrial dimensions are selectively disfavored, potentially due to the physical constraints imposed by the cellular environment or lipid droplet interference within white adipocytes. This concept aligns with previous observations in brown adipocytes, where the geometric arrangement of numerous lipid droplets allows for greater mitochondrial size increase or mitochondrial density compared to white adipocytes, which typically contain a single, large lipid droplet that limits available space for mitochondrial growth¹⁶. Understanding these constraints may require further investigation into the biochemical and structural factors that contribute to this selective exclusion and its impact on mitochondrial function.

Mitochondrial volume dynamics and structural limits

The determination of mitochondrial volume based on length and thickness measurements offers deeper insights into the potential energy-generating capacity of mitochondria in different body conditions^{17–19}. As expected, the cachectic group exhibited the lowest average mitochondrial volume, consistent with a compromised metabolic state associated with severe undernutrition or energy deficiency^{13,16,20}. In contrast, both the overweight and

normal-weight groups exhibited similar mitochondrial volumes in the subcutaneous flank region ($0.028 \mu\text{m}^3$), possibly indicating a compensatory mechanism to meet increased energy demands in these conditions (Fig. 2b). This compensatory mechanism may involve adjustments in mitochondrial biogenesis or changes in mitochondrial dynamics, such as fusion and fission processes, which could help maintain energy homeostasis under different physiological states²¹. It is important to acknowledge that mitochondrial morphology in adipose tissue may be influenced by lactation stage due to changes in hormonal and metabolic demands. Although cows in our study were categorized by BCS, we note that some variation in lactation status existed within groups (e.g., dry, mid-lactation, late lactation; see Table 2). However, this distribution was relatively balanced across groups and was not the primary factor used for stratification. Our objective was to investigate the relationship between mitochondrial size and body condition, independent of precise lactation timing. Nevertheless, we recognize that lactation stage could act as a confounding variable and future studies should control for or specifically assess its effect on adipocyte mitochondrial dynamics.

While the present study categorized animals by BCS, it is important to acknowledge that lactation stage may act as a confounding variable, particularly since all cachectic cows were dry, whereas cows in the normal and overweight groups were in lactating or post-calving stages (Table 2). While physiological status (lactating vs. dry) was not uniformly distributed among BCS groups, this distribution reflects biological constraints — cows in severe cachectic states are typically non-lactating due to energy depletion. Thus, physiological status may not be an independent confounder, but rather a manifestation of the extreme metabolic condition associated with low BCS. Additionally, while the number of animals per group was limited to three, each contributed multiple anatomical samples and hundreds of organelle-level measurements, which provided a high-resolution dataset suitable for identifying structural trends. Future studies should also incorporate physiological biomarkers such as non-esterified fatty acids (NEFA), β -hydroxybutyrate, glucose, or insulin levels to more precisely capture short-term metabolic states alongside structural observations. Additionally, with larger, physiologically stratified cohorts are warranted to disentangle the effects of BCS from lactation stage. Due to the limited number of animals per group and per anatomical region, our statistical analysis did not include a formal BCS \times Fat depot interaction term. Instead, we focused on examining main effects and consistent morphological trends. Future studies employing factorial designs with larger sample sizes are necessary to explore potential interactions between body condition and adipose depot. Moreover, longitudinal studies using serial fat biopsies from the same animals at different physiological stages may offer direct insight into the temporal dynamics of mitochondrial remodeling and enhance within-subject statistical robustness. Lactation is known to influence

Groups according to BCS values (1–5)*	Lactation period	Subcutaneous - flank area	Perirenal
Cachectic group (BCS = 1–2.33)			
Cow 9780 (BCS = 1.9) DMI: 12.5 kg/day ADG: -0.15 kg/day (weight loss)	Dry cow MY: 0 L/day	9780 A (5.0 g)	9780 B (5.1 g)
Cow 2156 (BCS = 1.6) DMI: 11.8 kg/day ADG: -0.20 kg/day (weight loss)	Dry cow MY: 0 L/day	2156 A (4.4 g)	2156 B (3.5 g)
Cow 6854 (BCS = 2.1) DMI: 13.0 kg/day ADG: -0.10 kg/day (weight loss)	Dry cow MY: 0 L/day	6854 A (3.3 g)	6854 B (4.0 g)
Normal weight group (BCS = 2.33–3.66)			
Cow 7886 (BCS = 3.1) DMI: 18.2 kg/day ADG: 0.30 kg/day	Late lactation MY: 26.5 L/day	7886 A (5.0 g)	7886 B (4.7 g)
Cow 2236 (BCS = 3.0) DMI: 17.9 kg/day ADG: 0.25 kg/day	Mid lactation MY: 24.8 L/day	2236 A (4.5 g)	2236 B (4.9 g)
Cow 7774 (BCS = 3.3) DMI: 18.5 kg/day ADG: 0.28 kg/day	Dry cow MY: 0 L/day	7774 A (4.8 g)	7774 B (4.2 g)
Overweight group (BCS = 3.66–5)			
Cow 5740 (BCS = 4.3) DMI: 21.0 kg/day ADG: 0.50 kg/day	Mid lactation MY: 22.3 L/day	5740 A (3.7 g)	5740 B (4.1 g)
Cow 2921 (BCS = 5.0) DMI: 20.5 kg/day ADG: 0.45 kg/day	Late lactation MY: 20.9 L/day	2921 A (4.6 g)	2921 B (3.6 g)
Cow 8646 (BCS = 4.9) DMI: 20.8 kg/day ADG: 0.48 kg/day	Post-calving MY: 21.5 L/day	8646 A (4.1 g)	8646 B (3.9 g)

Table 2. Cow groups selected by body condition score. ADG, Average Daily Gain; DMI, Daily Dry Matter Intake; MY, Milk Yield. The table shows the use of nine animals equally distributed among three groups. The four-digit numbers are the cow tags that represent the unique identifiers for each animal. An interval was calculated for each group, according to eq. 1, namely: cachectic group (BCS = 1–2.33), normal weight group (BCS = 2.33–3.66) and the overweight group (BCS = 3.66–5). The columns corresponding to the anatomical areas also show the measured weight (grams) of the adipose tissue samples.

mitochondrial dynamics through hormonal and metabolic shifts; however, our primary goal was to assess how mitochondrial morphology correlates with body condition—a variable that itself integrates both nutritional history and lactation-associated energy demands. Future studies should aim to incorporate lactation stage as an independent factor or control for it more rigorously to clarify its specific influence on adipocyte mitochondria.

These volume dynamics suggest that mitochondria are highly adaptable organelles capable of adjusting their size and possibly their functional capacity in response to varying metabolic demands and adipocyte states. White adipocytes in cows are specialized for long-term energy storage and are often characterized by a single large lipid droplet and low mitochondrial density²². The increase in size and volume of adipocyte mitochondria appears to have defined structural limits beyond which further growth may be restricted by mechanical stress from the lipid droplet, suggesting a delicate balance between lipid storage and mitochondrial function (Fig. 2b; Table 1). This contrasts with brown adipocytes, which, due to their geometry and higher number of smaller lipid droplets, can accommodate a greater mitochondrial density and expansion to support thermogenesis^{11,22,23}. Understanding these mechanical and structural constraints is crucial for appreciating how mitochondrial dynamics contribute to cellular homeostasis and energy regulation in white adipocytes¹². Thus, our study reveals a complex interplay between mitochondrial size, volume dynamics, and body condition in cow adipocytes, highlighting the importance of mitochondrial adaptability in maintaining energy homeostasis under different physiological states. The identification of size constraints and the observed exclusion zone within the mitochondrial population suggest selective processes that may influence metabolic efficiency and cellular health.

Mitochondria as regulators of metabolic health

Mitochondria play a central role in the regulation of metabolic processes in adipocytes by orchestrating the biochemical pathways involved in glucose and lipid metabolism, energy production via oxidative phosphorylation, and ATP synthesis^{7,8,10,24}. Given that mitochondrial function can influence insulin sensitivity and adipokine production (e.g., adiponectin)^{16,24–26}, variations in mitochondrial morphology have been associated with changes in cellular metabolism. The low mitochondrial content typically observed in white adipocytes underlines the importance of efficient mitochondrial organization in these cells to manage energy balance and adapt to metabolic demands²⁷. In this context, our findings highlight structural differences in mitochondria across BCS groups and adipose depots. While our study did not assess functional parameters directly, the observed morphological variation may support future investigations into the role of mitochondrial structure in adipocyte metabolic flexibility and systemic energy regulation^{26,28,29}.

The need for further studies

While our study provides insights into the morphological and volumetric properties of adipocyte mitochondria, it also underscores the need for more in-depth research to elucidate the molecular mechanisms driving mitochondrial size regulation, biogenesis, and functional specialization in white adipose tissue. Future studies should explore the potential role of pharmacological agents, such as PPAR-γ antagonists, in modulating mitochondrial biogenesis and function in white adipocytes, as well as the genetic and environmental factors that influence these processes^{14,16,21,30}. Additionally, more comprehensive investigations involving biochemical analyses and functional assays are needed to clarify the relationship between mitochondrial dynamics and systemic metabolic health, especially in the context of insulin resistance and obesity^{15,23}. Please note that while the study provides insights into mitochondrial size dynamics, it is important to consider the potential biases introduced by analyzing mitochondria in 2D sections, which may affect the measurement of length and thickness depending on the cutting plane. Future studies utilizing 3D imaging techniques, such as electron tomography, are needed to validate these findings. Furthermore, our discussion aligns with existing literature that suggests mitochondrial dynamics are closely linked to adipocyte metabolic functions (e.g.¹⁷), yet it remains speculative without supporting molecular data, such as mRNA expression or metabolic biomarkers. Although alterations in mitochondrial morphology have been associated with metabolic disease in other contexts, our current data do not allow us to establish any mechanistic or pathological link in dairy cows.

Materials and methods

This study involved the use of nine animals, namely three groups of Holstein dairy cows classified based on their Body Condition Score (BCS): (i) a cachectic group, (ii) a normal weight group, and (iii) an overweight group (Table 2). Adipose tissue samples (1 mm³) from two relevant anatomical regions have been collected for the analysis of mitochondria, namely the subcutaneous region of the flank and the kidney area. Please note that all experimental protocols were approved by the Department of Pathology licensing committee from Faculty of Veterinary Medicine, University of Agronomic Sciences and Veterinary Medicine, Romania. The methods used here were carried out in accordance with relevant guidelines and regulations. Average Daily Gain (ADG) was calculated as the difference between final and initial body weight divided by the number of days between the two measurements:

$$ADG = \frac{(Final\ weight - Initial\ weight)}{Number\ of\ days}$$

Body weight values were obtained from the recorded logs of the farm, and the interval used for each animal was based on the most recent available weight entries prior to sampling.

Body condition score

The BCS in cows lacks a universally accepted standardization^{20,31}. Two ways of numbering the BCS are used in the calving of cattle: (a) The Scottish/Canadian system (used mainly for dairy cows) uses a numbering from 1

to 5, with divisions of 0.25 units¹⁹. In this animal assessment system, most cows have a BCS of at least 2.5 and a maximum of 3. (b) The American system (used for beef cows) uses a numbering from 1 to 9, with divisions of one unit. In dairy farms most cows have BCS=5. When BCS=1 the animal is cachectic, and if BCS=9 the animal is overweight; were both situations are not desired in farms. If there are large differences between the values of the BCS, then the energy balance of the body is also affected¹⁷. If BCS is below 2.5 the animal cannot reach its productive potential because some of the ingested nutrients are directed to support the body, and if BCS is above 3, milk production also decreases because the ingested nutrients are directed towards increasing muscle and fat deposits^{18,32}. For our study we used the Scottish/Canadian system, where the BCS scale was divided into three parts, each part covering 2.33 divisions. We devised an equation that can be generalized to uniformly organize the animal population into groups, regardless of the type of BCS system used:

$$G(n) = Min + \frac{(Max - Min)}{Number\ of\ Groups} \times n$$

where *Min* is the minimum BCS value (1), *Max* is the maximum value (5), *Number of Groups* is the total number of BCS categories (3), and *n* is the group index (1 for cachectic, 2 for normal weight, 3 for overweight). In our case, *Max* was BCS=5, *Min* was BCS=1 and *n* was the group (*n*=1, the cachectic group, spanning 1–2.33; *n*=2, the normal weight group, spanning 2.33–3.66; and *n*=3, the overweight group, between 3.66 and 5). In short, the *Min* value subtracted from the *Max* value provides the BCS interval (1–5), which is further divided by the total number of groups (Table 2). This result is multiplied by each specific group to calculate the borders between the groups. In the final computation, the *Min* value is added to this result to offset the scale in the BCS interval. Thus, cattle were morphologically evaluated and their individual BCS values were matched to one of three groups based on their placement over these intervals (Fig. 1).

To classify the animals into three morphologically distinct groups (cachectic, normal weight, and overweight), we applied a linear interval partitioning method based on the Scottish/Canadian BCS scale, which ranges from 1 to 5. The total BCS interval (*Max* – *Min*) was 4 units (5–1=4), and this was divided into three equal subintervals to generate the group boundaries. Each group therefore spans 1.33 units.

$$Interval\ width = \frac{(Max - Min)}{Number\ of\ Groups} = \frac{(5 - 1)}{3} = 1.33$$

$$Upper\ boundary\ for\ Group\ n = Min + Interval\ width \times n$$

$$Group\ 1 = 1 + 1.33 \times 1 = 2.33$$

$$Group\ 2 = 1 + 1.33 \times 2 = 3.66$$

$$Group\ 3 = 1 + 1.33 \times 3 = 4.99$$

This resulted in the following classification:

Group 1 (cachectic): BCS 1.00–2.33.

Group 2 (normal weight): BCS 2.34–3.66.

Group 3 (overweight): BCS 3.67–5.00.

This approach ensures equal spacing across the BCS scale and provides a consistent, objective basis for assigning animals to each group (Fig. 1; Table 2). The inclusion of cow tags, BCS intervals, and anatomical area measurements in our study ensured accurate sample identification, precise categorization, and detailed anatomical context. These elements provided a solid foundation for our research, allowing for meaningful insights into the relationship between mitochondrial populations, adipocyte expansion, and metabolic regulation within different body condition categories.

Tissue samples

The sampling of adipose tissue in cows was conducted following established protocols for bovine adipose tissue collection, as described in previous literature³³. Two anatomical regions, namely the subcutaneous depot of the flank and the perirenal area, were selected for tissue collection. Adipose tissue samples of approximately 3 cm³ were collected from each cow on the slaughter line. A small incision was made at each selected anatomical region to access the adipose tissue. Careful attention was given to avoid contamination and damage to surrounding structures. Adipose tissue samples were collected using sterile instruments, ensuring proper aseptic technique. Upon collection, the adipose tissue samples were handled with care to maintain their integrity. Thus, the samples were promptly immersed in a 10% formaldehyde solution to preserve their structure and then labeled with detailed information (Table 3). Preservation methods, such as storing the samples at low temperatures, were employed to maintain sample quality. Samples were stored at 4 °C until processing for electron microscopy. Throughout the sampling process, meticulous documentation was maintained. On the same day of collection, the adipose tissue samples were transported to the laboratory for further processing. Each main sample was divided to be used for both optical microscopy and electron microscopy analysis. Records included crucial information such as the cow's identification, date and time of sampling, anatomical region sampled, and any relevant observations or notes.

Ultrastructure of the adipocyte mitochondria

The analysis of the structure and ultrastructure of the adipose tissue was performed on material included in epoxy resin (Epon) according to the standard procedure of the Ultrastructural Pathology Laboratory within the

Inclusion of adipose tissue fragments in epoxy resin	Temperature	Time
Tissue fixation in 4% glutaraldehyde buffered with 0.1 M TCS. The adipose tissue was cut into cubes of about 1 mm3 to be properly fixed.	4 °C	min 4 h
Wash in 0.1 M TCS	4 °C	2×1 h
Post-fixation with 0.1 M osmium tetroxide	4 °C	1 h
Wash in 0.1 M TCS	4 °C	2×10–15 min
Dehydration using ethyl alcohol 30°	4 °C	15–30 min
Dehydration using ethyl alcohol 50°	4 °C	15–30 min
Dehydration using ethyl alcohol 70°	4 °C	15–30 min
Dehydration using ethyl alcohol 90°	4 °C	15–30 min
Dehydration using ethyl alcohol 96°	RT	2×15 min
Dehydration using ethyl alcohol 100°	RT	3×15 min
Propylene oxide	RT	2×15 min
Bath I: Propylene oxide / epoxy resin (2/1)	RT	2 h
Bath II: Propylene oxide / epoxy resin (1/2)	RT	over night
Bath III: Epoxy resin in uncovered containers (to evaporate the remaining propylene oxide)	RT	2–3 h
Inclusion in epoxy resin in labeled plastic capsules	RT	–
Polymerization of epoxy resin	60 °C	48 h

Table 3. Processing adipose tissue fragments technique for ultrastructural analysis. This table outlines the detailed steps involved in processing adipose tissue fragments from dairy cows for ultrastructural analysis using electron microscopy. The table provides a sequential description of the Preparation method, beginning with the fixation of tissue samples in a 2.5% glutaraldehyde solution to preserve cellular structures, followed by rinsing in a buffer solution to remove excess fixative. The samples are then post-fixed in 1% osmium tetroxide, which enhances membrane contrast, before undergoing a series of graded ethanol dehydration steps to remove water content. The dehydrated samples are subsequently infiltrated with and embedded in a resin to maintain their ultrastructure integrity during sectioning. Ultrathin sections are cut with an ultramicrotome and then mounted on copper grids. The sections are then contrasted with uranyl acetate and lead citrate to improve electron density, facilitating the visualization of mitochondria and other organelles under the electron microscope. This protocol ensures high-quality imaging for detailed examination of adipocyte mitochondrial morphology and other cellular structures. Please note that “RT” means room temperature.

“Victor Babeş” National Institute. Examination of the tissue fragments was carried out in the first stage on optical microscope sections of 1 µm for histological evaluations done with Toluidine Blue.

Once the overall optical microscope assessment was made, the next step consisted of ultrafine sections for the electron microscopic evaluation that was required for the final steps of the study. Ultrafine sections were cut using a diamond knife at 60–80 nm, double-stained with 1% uranyl acetate and lead citrate (Reynolds solution). Sectioning was performed with an MTXL RMC ultramicrotome (Boeckeler Instruments Inc., USA), and the examination was made using an 80 kV Morgagni 268 TEM transmission electron microscope (FEI Company, The Netherlands). Relevant images were acquired using a MegaView III CCD at 0.5 µm, 1 µm and 2 µm magnification. Image processing was performed using the iTEM-SIS software (Olympus, Germany). All measurements were made with the same digital image processing software. It should be noted that only mitochondria with clearly visible cristae were measured. The length and thickness measurements have taken into account the positioning of the cristae. The length was measured on the axis that was perpendicular to the cristae and the thickness was measured on the axis that was parallel to the cristae. Electron micrographs were analyzed using *ImageJ* software (NIH, USA), where mitochondrial length and thickness were measured manually. The rough volume of adipocyte mitochondria was calculated using the formula: $V = \pi r^2 h$. Where r is the radius represented by the width of a cylinder divided in half (thickness/2) and h is represented as the cylinder height. Here, the width was represented by the thickness of the mitochondria, and the height was represented by the length of the mitochondria on the electron-microscopy image. A series of well-known equations have been used to compute the results (Table 4).

Equation 1 allowed the organization of dairy cows into groups, based on their individual BSC score (Table 4; Eq. 1). Following the sampling, processing and morphometric measurements of mitochondria populations in adipocytes, descriptive statistical values were calculated such as: mean, standard deviation and variance (Table 4; with the help of Eqs. 2, 3 and 4). Also, the approximate volume of each mitochondrion was calculated by applying the formula for the volume of the cylinder (Table 4; Eq. 5). Additionally, the coefficient of variation was further used to describe the dynamics of mitochondria (Table 4; Eq. 6).

No.	Purpose	Equation
1	Calculation of group intervals over the BCS scale.	$G(n) = Min + \frac{(Max - Min)}{no. groups} \times n$
2	Calculation of mean value.	$\bar{x} = \frac{\sum_{i=1}^n x_i}{n}$
3	Calculation of standard deviation.	$\sigma = \sqrt{\frac{\sum_{i=1}^n (x_i - \bar{x})^2}{n - 1}}$
4	Calculation of variance.	$v = \frac{\sum_{i=1}^n (x_i - \bar{x})^2}{n - 1}$
5	The rough volume of adipocyte mitochondria.	$V = \pi \times r \times 2 \times h$
6	Calculation of the Coefficient of Variation (CV%). It shows the highest variation among a set of values.	$CV\% = \frac{\sigma}{\bar{x}} \times 100$

Table 4. List of equations. The table unfolds all equations used to process the Raw data resulting from the experiments. The variables used here to store the results of the analysis have the following meaning: group partition (G(n)), mean value (x), standard deviation (σ), variance (v), coefficient of variability (CV%).

Data availability

Data is provided within the manuscript or supplementary information files.

Received: 1 February 2025; Accepted: 21 July 2025
Published online: 13 August 2025

References

1. Soubrier, J. et al. Early cave Art and ancient DNA record the origin of European bison. *Nat. Commun.* **18** (7), 13158 (2016).
2. Pitt, D. et al. Domestication of cattle: Two or three events? *Evol. Appl.* **12** (1), 123–136 (2018).
3. Orozco-terWengel, P. et al. Revisiting demographic processes in cattle with genome-wide population genetic analysis. *Front. Genet.* **6**, 191 (2015).
4. Zhang, K., Lenstra, J., Zhang, S., Liu, W. & Liu, J. Evolution and domestication of the bovine species. *Anim. Genet.* **51** (5), 637–657 (2020).
5. Wilhelm, K. Re-thinking dairy cow feeding in light of food security. *AgroLife Sci. J.* **2** (1), 36–40 (2013).
6. Sauerwein, H., Bendixen, E., Restelli, L. & Cecilian, F. The adipose tissue in farm animals: A proteomic approach. *Curr. Protein Pept. Sci.* **15** (2), 146–155 (2014).
7. Yu, S. & Pekkurnaz, G. Mechanisms orchestrating mitochondrial dynamics for energy homeostasis. *J. Mol. Biol.* **430** (21), 3922–3941 (2018).
8. Depaoli, M., Hay, J., Graier, W. & Malli, R. The enigmatic ATP supply of the Endoplasmic reticulum. *Biol. Rev. Camb. Philos. Soc.* **94** (2), 610–628 (2019).
9. Kowal, J., Yegutkin, G. & Novak, I. ATP release, generation and hydrolysis in exocrine pancreatic duct cells. *Purinergic Signal.* **11** (4), 533–550 (2015).
10. Neupane, P., Bhujar, S., Thapa, N. & Bhattarai, H. ATP synthase: Structure, function and Inhibition. *Biomol. Concepts.* **10** (1), 1–10 (2019).
11. Pollard, A. & Carling, D. Thermogenic adipocytes: Lineage, function and therapeutic potential. *Biochem. J.* **477** (11), 2071–2093 (2020).
12. Shao, M. & Gupta, R. Transcriptional brakes on the road to adipocyte thermogenesis. *Biochim. Biophys. Acta Mol. Cell. Biol. Lipids.* **1864** (1), 20–28 (2019).
13. Coman, A., Nicolae, S., Codreanu, I. & Crivineanu, M. Comparative study regarding the protein, energy and mineral profiles in the different categories of intensive and household bred cattle. *Sci. Works Ser. C Vet. Med.* **LXVIII**(2), 13–16 (2022).
14. Wang, D. et al. FOXO1 Inhibition prevents renal ischemia–reperfusion injury via cAMP-response element binding protein/PPAR-γ coactivator-1α-mediated mitochondrial biogenesis. *Br. J. Pharmacol.* **177** (2), 432–448 (2020).
15. Honecker, J. et al. A distribution-centered approach for analyzing human adipocyte size estimates and their association with obesity-related traits and mitochondrial function. *Int. J. Obes. (Lond).* **45** (9), 2108–2117 (2021).
16. Lee, J. et al. The role of adipose tissue mitochondria: Regulation of mitochondrial function for the treatment of metabolic diseases. *Int. J. Mol. Sci.* **20** (19), 4924 (2019).
17. Roche, J., Kay, J., Friggens, N., Loo, J. & Berry, D. Assessing and managing body condition score for the prevention of metabolic disease in dairy cows. *Vet. Clin. North. Am. Food Anim. Pract.* **29** (2), 323–336 (2013).
18. Roche, J. et al. Invited review: Body condition score and its association with dairy cow productivity, health, and welfare. *J. Dairy Sci.* **92** (12), 5769–5801 (2009).
19. Sakaguchi, M. Differences between body condition scores and body weight changes in postpartum dairy cows in relation to parity and reproductive indices. *Can. Vet. J.* **50** (6), 649–656 (2009).
20. Kadokawa, H. & Martin, G. A new perspective on management of reproduction in dairy cows: The need for detailed metabolic information, an improved selection index and extended lactation. *J. Reprod. Dev.* **52** (1), 161–168 (2006).
21. De Pauw, A., Tejerina, S., Raes, M., Keijer, J. & Arnould, T. Mitochondrial (dys)function in adipocyte (de)differentiation and systemic metabolic alterations. *Am. J. Pathol.* **175** (3), 927–939 (2009).
22. Stanford, K. et al. Brown adipose tissue regulates glucose homeostasis and insulin sensitivity. *J. Clin. Invest.* **123** (1), 215–223 (2013).
23. Maliszewska, K. & Kretowski, A. Brown adipose tissue and its role in insulin and glucose homeostasis. *Int. J. Mol. Sci.* **22** (4), 1530 (2021).
24. Koh, E. et al. Essential role of mitochondrial function in adiponectin synthesis in adipocytes. *Diabetes* **56** (12), 2973–2981 (2007).
25. Mendham, A. et al. Exercise training results in depot-specific adaptations to adipose tissue mitochondrial function. *Sci. Rep.* **10** (1), 3785 (2020).

26. Woo, C., Jang, J., Lee, S., Koh, E. & Lee, K. Mitochondrial dysfunction in adipocytes as a primary cause of adipose tissue inflammation. *Diabetes Metab. J.* **43** (3), 247–256 (2019).
27. Sun, K., Kusminski, C. & Scherer, P. Adipose tissue remodeling and obesity. *J. Clin. Invest.* **121** (6), 2094–2101 (2011).
28. Wang, Y. et al. Improvement of obesity-associated disorders by a small-molecule drug targeting mitochondria of adipose tissue macrophages. *Nat. Commun.* **12** (1), 102 (2021).
29. Gubceac, E., Gaita, L., Gagniuc, P. & Militaru, M. Fractal characteristics of adipocyte dynamics in mice. *Sci. Works Ser. C Vet. Med.*, **LXI**(1), 51–56 (2015).
30. Szendroedi, J., Phielix, E. & Roden, M. The role of mitochondria in insulin resistance and type 2 diabetes mellitus. *Nat. Rev. Endocrinol.* **8**, 92–103 (2011).
31. Edmonson, A., Lean, J., Weaver, L., Farver, T. & Webster, G. A body condition scoring chart for Holstein dairy cows. *J. Dairy. Sci.* **72**, 68–78 (1989).
32. Olteanu, M. et al. Volcanic tuff, potential source of minerals in dairy cows feeding. *AgroLife Sci. J.* **8**(1), 206–213 (2019).
33. Mann, S. Symposium review: The role of adipose tissue in transition dairy cows: Current knowledge and future opportunities. *J. Dairy. Sci.* **105** (4), 3687–3701 (2022).

Acknowledgements

None.

Author contributions

E.G. carried out the experiment, performed the measurements, developed the theoretical formalism. E.G. and A.M.P. conducted the analytic calculations. E.G. wrote the manuscript with support from M.M., A.M.P. and M.G., who also helped supervise the project. E.G. and M.M. conceived the original idea, with M.M. overseeing the overall project direction and execution. D.I.N. contributed to the development and application of statistical methods and artificial intelligence models used for data analysis, while P.A.G. provided expertise in advanced statistical analysis and helped refine the statistical approaches applied in the study. The collaborative efforts ensured a comprehensive investigation of mitochondrial dynamics in adipose tissue. All authors reviewed the manuscript.

Funding

Not applicable.

Declarations

Competing interests

The authors declare no competing interests.

Ethics approval

Not applicable.

Generative AI and AI-assisted technologies in the writing process

Not applicable.

Additional information

Correspondence and requests for materials should be addressed to A.-M.P., D.-I.N. or P.A.G.

Reprints and permissions information is available at www.nature.com/reprints.

Publisher's note Springer Nature remains neutral with regard to jurisdictional claims in published maps and institutional affiliations.

Open Access This article is licensed under a Creative Commons Attribution-NonCommercial-NoDerivatives 4.0 International License, which permits any non-commercial use, sharing, distribution and reproduction in any medium or format, as long as you give appropriate credit to the original author(s) and the source, provide a link to the Creative Commons licence, and indicate if you modified the licensed material. You do not have permission under this licence to share adapted material derived from this article or parts of it. The images or other third party material in this article are included in the article's Creative Commons licence, unless indicated otherwise in a credit line to the material. If material is not included in the article's Creative Commons licence and your intended use is not permitted by statutory regulation or exceeds the permitted use, you will need to obtain permission directly from the copyright holder. To view a copy of this licence, visit <http://creativecommons.org/licenses/by-nc-nd/4.0/>.

© The Author(s) 2025